Near-Far Effect on Coded Slotted ALOHA

Ehsan Ebrahimi Khaleghi, Cédric Adjih, Amira Alloum, Paul Mühlethaler

Near-Far Effect on Coded Slotted ALOHA

Ehsan Ebrahimi Khaleghi*, Cedric Adjih*, Amira Alloum§ and Paul Mühlethaler*
*Inria, Université Paris-Saclay, France
Email: <FirstName>.<FamilyName>@inria.fr
§Nokia Bell-labs, France
Email: amira.alloum@nokia-bells-labs.com

***Abstract*—Motivated by scenario requirements for 5G cellular networks, we study one of the candidate protocols for massive random access: the family of random access methods known as Coded Slotted ALOHA (CSA). A recent trend in research has explored aspects of such methods in various contexts, but one aspect has not been fully taken into account: the impact of path loss, which is a major design constraint in long-range wireless networks. In this article, we explore the behavior of CSA, by focusing on the path loss component correlated to the distance to the base station. Path loss provides opportunities for capture, improving the performance of CSA. We revise methods for estimating CSA behavior, provide bounds of performance, and then, focusing on the achievable throughput, we extensively explore the key parameters, and their associated gain (experimentally). Our results shed light on the behavior of the optimal distribution of repetitions in actual wireless networks.**

I. Introduction: Motivation and Related Work

One of the main challenges for the fifth generation of wireless standards is simultaneous support for the requirements of diverse Internet of Things (IoT) scenarios: high spectral efficiency, very low latency and highest reliability, with massive deployment handling tens of billions of monitoring and controlling devices by 2025. This leads to a critical variability of key constraints such as payload size and targeted delays. Consequently among the current challenges [1], we can cite :

- Connectionless transmissions: reducing the control signaling (overhead, collision resolution, latency) of random access procedures for massive connectivity.
- Grant-less transmissions: reducing the control and grant signaling of resource allocation and scheduling requests in the multiple-access procedures.
- Finite blocklength regimes: reducing decoding delays and signaling by handling transmission and coding mechanisms for very short packets.

These requirements challenge present coding strategies, as well as the multiple and random access mechanisms used in the current wireless standard LTE/LTE-A, involving an important amount of signaling, delays and overhead (PRACH/Scheduling Request procedure).

Coding techniques are a key enabler to realize many of the above challenges and in particular the grant-less and connectionless random access procedure for IoT applications. Among promising approaches to achieve this goal, non orthogonal multiple access (NOMA) [2] is known to accommodate the device tsunami via non orthogonal resource allocation using the code domain multiplexing and a particular grant less random access procedure. Some existing physical layer solutions are limited by scalability and complexity issues.

A more practical alternative consists in designing new efficient connectionless access protocols for small bursty transmissions, since that within the existing cellular standard (LTE) any connection oriented approach involves establishing a bearer prior to data transmission, which is inefficient for small burst traffic due to the signaling involved [3]. This alternate avenue has been explored by the family of methods known as Coded Slotted ALOHA (CSA), and extensively studied in the last decade. These methods include: Contention Resolution Diversity Slotted ALOHA (CRDSA) in [4], Irregular Repetition Slotted ALOHA (IRSA) in [5], Coded Slotted ALOHA (CSA) in [6], [7]. It consists in retransmitting replicas of each packet (possibly with a predefined error correcting scheme), and introducing the mechanism of physically and successively removing the signal of every packet that has been successfully retrieved at the position of its replicas.

In our setting, we propose to include path loss in the model of CSA, and to take into account captures through the near-far effect. We evaluate the performance and the benefits. Indeed, the effect of path loss and fading in wireless networks has been widely analyzed (for instance through stochastic geometry as in [8]), along with the performance of capture and successive interference cancellation receivers for Slotted ALOHA protocols [9]–[12]. Yet it has not been completely covered coupled with the coding and information theory aspects dominating in Coded Slotted ALOHA for short payloads [1]. The references [13] and [14] are the closest to our assumptions, but they focus exclusively on users experiencing channels with identical statistics (i.i.d Rayleigh fading). In the present paper, we propose a study of CSA in the context of path loss (correlated to distance) and capture for interference-limited cellular networks. The main open questions related to our model are: How much gain can be achieved in terms of throughput when capture is performed? What is the maximum achievable throughput for CSA under the capture effect? What would be the optimal repetition distribution? We go some way to providing answers, and among other results, we show the enduring good performance of the Soliton [15] distribution with representative network parameters.

The article is organized as follows: Section II introduces the concepts of CSA, path loss and capture effect with the related notations and models. Then, Section III describes how the *density evolution* method enables the performance evaluation

for CSA. Section IV introduces an upper bound for the throughput. Afterwards, Section V discusses the performance of CSA in the wireless model considered, mostly through simulations, comparison with bounds, and density evolution evaluation. Conclusions are given in Section VI.

II. Model, Notations and Problem Formulation

A. Coded Slotted Aloha : Background and Notations

We consider a cellular IoT network with a massive deployment of M user nodes contending for a connectionless random access to a base-station over a frame of N *time slots* (referred to as *slots*). The transmission of a single packet matches the duration of a slot.

1) CSA Operation: Given the well-known performance limitations of the slotted Aloha protocol, diversity through the use of repetition coding has been widely studied in slotted Aloha protocols [16] [7]. They also are at the basis of CSA protocols, which additionally, introduce innovative decoding techniques described later.

We use the CSA variant of [5] (IRSA), but we will refer to it as CSA in the rest of the article (consistent with the literature): at the beginning of the frame, each of the M users selects a random repetition factor d according to some predefined distribution (denoted L later). The node then sends d replicas of the packet over d randomly and independently chosen slots[1].

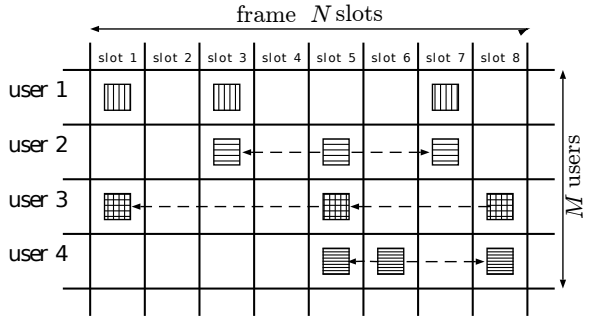

Fig. 1: Frame of size $N = 8$, and $M = 4$ users. Decoding is possible in 4 iterations: slot 6 yields the packet of user 4, slot 8 then yields the packet of user 3, slot 5 then yields the packet of user 2, and finally the packet of user 1 is retrieved on any of the slots 1, 3 or 7

The decoding of CSA is based on the idea, introduced in CRDSA [4], that each packet contains pointers, that indicate the other slots in the frame where each replica of the same packet is transmitted. This allows iterative decoding as follows: when a packet is the only transmission that occurred in a slot, a *singleton* (for instance, the packet of user 4 on slot 6 in Fig. 1), then it can be decoded without any "collisions" with other users. The novelty of CRDSA, is that once a singleton packet is decoded, the number and the position of the other replicas are known using its pointers. Hence, that packet replicas are *physically* subtracted from all the slots where they are known to have been transmitted (in Fig. 1, packet of user 4 is subtracted from slots 5 and 8). Consequently, new singleton packets can appear in these slots (packet from user 3 in slot 8 in Fig. 1), and the process is iterated until all the packets are retrieved or no progress is made.

When a packet is recovered in a singleton slot, it is re-encoded and re-modulated then the receiver removes its interference contribution from future $d-1$ slots, where replicas are located, and this process is akin to the technique known as *successive interference cancellation* (SIC) [9]. As the sucessful singleton transmission and the interference cancellation are done in different slots rather than the same slot, we refer to the receiver decoding scheme as *inter-slot SIC*.

2) CSA Decoding Analysis: The analogy based on iterative error correcting codes has been introduced in the seminal work of Liva [5] to model the iterative collision resolution with modern coding theory tools. Accordingly, the problem of uncoordinated multiple access has been extensively studied over the last decade using the code-on-graph model iteratively decoded over an erasure channel [15]. The model is based on considering user nodes as variable nodes and slots as parity check nodes of a corresponding Tanner graph. For instance,

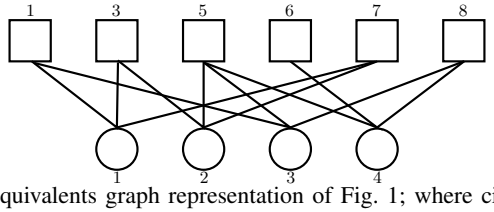

Fig. 2: Equivalents graph representation of Fig. 1; where circles are *variable nodes* representing users and squares are *parity check nodes* representing slots.

Fig. 2 represents the Tanner graph related to Fig. 1: square 1 is connected to circles 1 and 3 because users 1 and 3 both transmitted in slot 1, and circle 1 is connected to square 1, 3 and 7 because user 1 transmitted in slots 1, 3 and 7. We use the terminology *user node* and *slot node* to refer to the two nodes population on the Tanner graph. Using notations of classical coding theory, the polynomial representation of the user then slot node-degree distributions are respectively expressed as $L(x) = \sum_i L_i x^i$ and $R(x) = \sum_i R_i x^i$. The corresponding edge distributions are respectively denoted as $\lambda(x) = \sum_i \lambda_i x^i = \frac{L'(x)}{L'(1)}$ and $\rho(x) = \sum_i \rho_i x^i = \frac{R'(x)}{R'(1)}$.

The distribution L is selected by the protocol designer: L_i represents the probability that one given user chooses to transmit exactly i replicas in the frame. The regular and the irregular distribution cases have been considered, and the Soliton distribution has been demonstrated to be optimal in terms of throughput efficiency in [15] when $N \to \infty$. L directly defines the distribution R, through the fact that the slots are selected uniformly i.i.d. by the user. Hence R follows a binomial distribution $B(N, \frac{R'(1)}{M})$.

In coding terms, the process of decoding in done as follows. Each collision occurring at a slot, satisfies a parity check equation containing as many erased variables as unknown packets

[1]Note that in the prior variant CRDSA of [4], nodes were sending packets a fixed number of times $d = 2$. The corresponding discrete distribution L is defined as $L_2 = \Pr(d = 2) = 1$ and for $i \neq 2, L_i = Pr(d = i) = 0$, noted $L(x) = x^2$ using notation introduced later. IRSA generalizes this to an arbitrary distribution; the reason being that better performance can achieved when all users do not send the same amount of replicas.

colliding within the slot considered. At each slot, the belief propagation algorithm [17] is performed at the receiver in order to resolve the collisions. Let us notice that in the particular case of the erasure channel the belief propagation algorithm is equivalent to the inter-slot SIC decoding algorithm where a packet recovery is possible if and only if that packet is the only one unknown in the parity check equation modeling the corresponding slot. Though the packets recovered or received in previous slots are taken into account using headers, the suboptimal belief propagation decoder declares a failure when a stopping set occurs on the Tanner graph [17]. The latter erasure patterns are a limiting factor for CSA performance.

We can remark that the erasure channel model together with the suboptimal SIC iterative receiver still limit the CSA performance below the maximum likelihood one. However the performance of the iterative collision resolution receiver can be enhanced by the phenomenon of capture that occurs naturally at the physical layer, as described in the next section.

B. Path Loss and Capture Model: Background and Notations

We propose to take into account the capture effect that can naturally occur and/or be induced (by modulation, and decoding techniques, e.g. multi-packet reception), in particular in the presence of path loss. This direction has been extensively studied in the slotted aloha literature with SIC, or multiple packet receivers [9]–[12], then more recently in the context of CSA in Rayleigh fading scenarios [13].

In our setting, we consider an interference limited cellular network and neglect the fading and the shadowing effect (constant channel), only considering the effect of path loss.

A power based capture happens on a packet when the signal-to-interference-plus-noise-ratio (SINR) involving concomitant transmitters is larger than the capture ratio. When noise is neglected only the signal to interference ratio (SIR) is considered.

We introduce the following notations and assumptions on the wireless network:

- We consider the nodes to be randomly uniformly distributed in a disk of radius 1.
- r_i is the distance of the user node i to the base station.
- α denotes the path loss exponent.
- $\beta > 0$ denotes the capture threshold and is determined by the properties of the communication system. In our setting we consider $\beta > 1$ as we study narrowband scenarios for IoT cellular systems (LTE, 5G).
- The received power for user node i is denoted $P_i = h_i \times r_i^{-\alpha}$ where h_i denotes the channel gain (excluding path loss) for the user node i. Fading and shadowing effects are not considered in the present work, thus we set $h_i = 1$.
- When K user nodes transmit simultaneously in a given slot, the SIR is: $\mathsf{SIR}_i = \frac{P_i}{\sum_{j=1, j\neq i}^{K} P_j} = \frac{r_i^{-\alpha}}{\sum_{j=1, j\neq i}^{K} r_j^{-\alpha}}$

Thus a packet transmitted by user node i is successfully captured when: $\mathsf{SIR}_i \geq \beta$

Once a packet has been captured in one slot, we assume that the base station is able to subtract from the same slot (since it is able to perform the more complex operation of inter-slot SIC anyway). This is SIC as it is classically defined [9], we call this *intra-slot* SIC.

C. Parameters and Performance Metrics

One of the most important parameters of the system is the load, defined as the average number of users per slot: $g = \frac{M}{N}$. The average number of repetitions per user is noted ℓ_{avg}, and the average number of user transmissions per slot is noted r_{avg}. We have $\ell_{\text{avg}} = L'(1)$, and $r_{\text{avg}} = R'(1) = g\ell_{\text{avg}}$.

The main metric in the evaluation of the performance is the throughput T, defined as the average proportion of retrieved packets per slot. T is a function of g, M and $L(x)$; obviously $T(g, M, L) \leq g$. It is also a function of the physical layer model: we denote T_{base} the throughput g for a model without capture as in [5] and T_{SIR} the throughput of g with our wireless network assumptions.

The behavior of the throughput is as follows: when the load g is small, all packets tend to be retrieved, hence $T(g) \approx g$. When g increases, the proportion of non-retrieved packets in the decoding process also increases, and T usually reaches a maximum, after which performance decreases due to overload.

For T_{base}, an absolute bound is $T_{\text{base}}(g) \leq 1$, since at most one packet can be retrieved per slot. The Soliton distribution asymptotically reaches this bound for $g \to 1$, and $N \to \infty$ [15].

III. Performance Analysis with Density Evolution

A. Density Evolution without intra-slot SIC (capture)

A form of *Density Evolution* (DE) [17] was introduced by Liva [5] for CSA using the analogy with decoding codes-on-graphs. It models the decoding process of the successive iterations of CSA by an equivalent iteration of functions applied to variables summarizing the state of the system, and ultimately yields, among other results, a numeric estimation of the throughput denoted $\mathcal{T}^{\text{DE}}$ ($\mathcal{T}^{\text{DE}}_{\text{base}}$ for the estimate of T_{base} obtained by DE and $\mathcal{T}^{\text{DE}}_{\text{SIR}}$ for the estimate of T_{SIR}).

Let us consider the representation as the Tanner graph in Fig. 2, and successively: the edges in the direction from slot nodes to user nodes (top to bottom in Fig. 2), noting p_i the probability that the edge has an associated slot node that is still unknown; and then the edges in the direction from user nodes to slot nodes (bottom to top), denoting q_i the probability of an unknown associated user node. Then a link between these probabilities can be established, as given by Equations (1) and (2) of [5], reproduced in our Eq. (1); they imply a recursive system:

$$q_i = \lambda(p_{i-1}) \text{ and } p_i = 1 - \rho(1 - q_i). \tag{1}$$

One can start with initial condition: $q_0 = 1$ (no known user nodes). Asymptotically (e.g. when $N \to \infty$, and with independence assumptions, in particular, the absence of loop in the graph that becomes a tree), this closely models the decoding process, and provides a tool for evaluating performance. We denote q_{lim} the value obtained after ending the iteration process; when it converges towards 0, asymptotically,

the user packets will be decoded with a probability close to 1. When it converges towards another fixed point > 0 only a corresponding fraction of the packets will be decoded. In any case, if further we denote $p_{lim} = 1 - \rho(1 - q_{lim})$, then the packet loss rate (proportion of non-retrieved packets) is obtained as $P_L = \Lambda(p_\infty)$. The estimate of the throughput is $\mathcal{T}^{\mathrm{DE}}_{\mathrm{base}}(g, M, L) = (1 - P_L)g$.

This model can be extended; for instance Appendix A of [5] updates it to account both for decoding errors (due to residual "noise" after a given number of inter-slot SIC), and for capture effects. Namely the recursion for p_i on the right of Eq. (1) is replaced by the following equation:

$$p_i = 1 - \sum_{\ell=0}^{\ell_{\max}} \rho_\ell \sum_{t=0}^{\ell-1} w_{\ell,t} \binom{\ell-1}{t} (1-q_i)^t q_i^{(\ell-1-t)}. \quad (2)$$

where $w_{\ell,t}$ is the probability that one packet can be recovered in a slot where ℓ simultaneous transmissions have been made, and after t packets have been removed (by intra-slot or inter-slot interference cancellation). $\ell_{\max}$ is simply such that $\rho_\ell = 0$ for $\ell \geq \ell_{\max}$, and $\ell_{\max} \leq M$.

B. Density Evolution with intra-slot SIC (capture)

An identical equation is the starting point for the study of the DE in the presence of capture in [13] (with different notations). There, however, $w_{\ell,t}$ is defined more precisely as: the probability that the outgoing edge corresponds to a user transmission that is recovered in one of the possible successive captures of the slot. [13] also further refines modeling for the specific case of Rayleigh fading, but without path loss, to provide analytic evaluations of $w_{\ell,t}$. A derivation of similar DE equations is also presented in [14] again in the context of block Rayleigh fading, with further analytic evaluations.

In our setting, we start with Eq. (2) and extend it to our model. To estimate $w_{\ell,t}$, we consider a slot where $i = \ell - t$ unrecovered simultaneous transmissions occur in a slot within our network model. Given the users' positions, taken as uniformly distributed random variables, a capture is likely to be successful on the strongest signal with a given probability. After one capture, inter-slot SIC is performed, then another capture is possible, and so on.

We denote $\mathcal{C}_i$ the average number of recovered packets among i simultaneous transmissions. Doing so, we adopt the approach of [14] whose equations 7 and 8 are recovered by equating $\mathcal{C}_i$ to their "$D(r)$". Whereas [14] derives "$D(r)$" as a closed-form expression depending directly on Rayleigh fading properties, we use Monte-Carlo estimations to compute this value[2] (see [11] for evaluating $\mathcal{C}_i$ analytically), and directly write: the probability that one pre-defined packet detection is successful among the successful captures occurring over the i concommitent transmissions is $\frac{1}{i}\mathcal{C}_i$. Then:

$$w_{\ell,\ell} = 0,\ w_{\ell,\ell-1} = 1,\ \text{and}\ w_{\ell,t} = \frac{\mathcal{C}_{\ell-t}}{\ell - t}\ \text{for}\ t \leq \ell - 2 \quad (3)$$

IV. Throughput Bounds

First we observe that CSA with capture will always decode more than without capture, hence a trivial lower bound of the throughput $T_{\mathrm{SIR}}(g)$ is the one given by $T_{\mathrm{base}}(g)$.

We now propose an upper bound g_0 for the load g in the lossless regime, and the associated maximum (lossless) throughput. We denote an *upper bound of lossless throughput*.

It is slightly less general than an upper bound, because actual performance might exceed that bound, at the expense of operating with losses. Note that it is still meaningful because it is more interesting to use CSA in the lossless regime (or at least with low loss rate) and also because, at least for T_{base}, performance can drop dramatically after leaving the lossless regime, leaving little room to exceed the bound.

The background is in the results of [5], [6] detailing the behavior of the DE for $\mathcal{T}^{\mathrm{DE}}_{\mathrm{base}}(g)$. Starting from $g = 0$, the DE yields a $q_{lim} = 0$ until some threshold $g = g^*$ is reached, and beyond which the DE no longer converges towards $q_{lim} = 0$. Accordingly, this yields $\mathcal{T}^{\mathrm{DE}}_{\mathrm{base}}(g) = g$ for $g \leq g^*$ and $\mathcal{T}^{\mathrm{DE}}_{\mathrm{base}}(g) < g$ beyond $g > g^*$. In other terms, the DE analysis (and therefore CSA when $N \to \infty$) shows that the decoding process is lossless until threshold g^* after which performance collapses.

Theorem 1. *The upper bound g_0 of the maximum load g^* up to which the network may operate without losses (asymptotically, when $N \to \infty$) and the associated transmission throughput bound for CSA with capture effect without losses are:*

$$g_0 = \frac{1}{(1-\gamma^2)},\ T_{\mathrm{lossless-upper-bound}} = \frac{1}{(1-\gamma^2)} \quad (4)$$

with $\gamma = \beta^{-\frac{1}{\alpha}}$. These bounds are independent of the node distribution $L(x)$.

Proof. Our common approach for establishing the bounds consists in considering nodes that either necessarily interfere with each other or conversely transmissions that are automatically captured (because of the near-far effect).

Let us denote $\mathrm{ann}(r_1, r_2)$ the ring (mathematically: annulus) represented by the set of points between the circle of radius r_1 and circle of radius r_2. Let us consider one slot with two simultaneous transmissions by users that are at distances respectively r_1 and r_2 from the base station with $r_1 \leq r_2$.

In our model, capture occurs iff the SIR verifies $\frac{r_1^{-\alpha}}{r_2^{-\alpha}} \geq \beta$ or equivalently $r_2 \geq \gamma^{-1} r_1$ where $\gamma = \beta^{-\frac{1}{\alpha}}$. That condition can never be satisfied if $\gamma^{-1} r_1 > 1$, because that would imply $r_2 > 1$, inconsistent with our hypothesis that transmitters are in the origin disk of radius 1. Hence transmissions by the nodes in the ring $\mathrm{ann}(\gamma, 1)$ can never be successfully captured when two (or more) of the nodes are transmitting simultaneously.

[2]Note that the behavior of path loss is qualitatively very different from Rayleigh fading: e.g. if we were in an infinite plane instead of a unit disk but with the same density (hence with an infinite number of simultaneous transmissions), the average number of recovered packets would be "$\mathbb{E}[N]$" of [12] for instance which is > 0. One could deduce that Slotted ALOHA with repetition coding and intra-slot SIC (a lower bound for CSA) in an unit disk has a throughput converging to a constant > 0 when the density converges to infinity.

Because there is no capture inside the ring, the throughput obtained when only nodes of that ring are transmitting, is given by T_{base} (and is an upper bound when other nodes transmit). The load g' in the ring is $g' = (1-\gamma^2)g$, since the ratio of the nodes in the ring to the nodes in the unit disk is $(1-\gamma^2)$.

We then observe that the throughput without capture $T_{\text{base}}(g')$ is bounded by 1, hence losses are guaranteed to occur whenever $g' \geq 1$. Thus a necessary condition for lossless transmissions is $(1-\gamma^2)g \leq 1$, yielding the bound $g \leq \frac{1}{(1-\gamma^2)}$. Our upper bound (of g^*) for lossless transmission is thus $g_0 = \frac{1}{(1-\gamma^2)}$, and the corresponding lossless throughput bound is $T_{\text{lossless-upper-bound}} = g_0 \geq T_{\text{SIR}}(g_0)$. □

V. Experimental Results

In this section, we explore the performance of the CSA in the presence of near-far effect through several evaluation tools: 1) simulations, 2) the bound in Eq. (4) and 3) density evolution. In the process, we compare simulation results, the bound, and DE results.

We follow a semi-systematic methodology where we start from one fixed configuration (see Section V-A), and evaluate the impact of various parameters, usually by changing one at a time. Occasionally, in order to better confirm some observations, further evaluation is performed by introducing some additional extra change.

A. Experimental Settings

We perform an experimental evaluation with custom Matlab and Python codes and appropriate scientific libraries.

Our reference configuration is given in Table I. This defines the values of the parameters, in the following sections, whenever there are not otherwise specified. The number of simulations is 1000 if all the results of a graph are for $N = 100$, and 100 otherwise.

	Parameter	Default value(s)
Wireless	Path loss exponent	$\alpha = 4$
	Capture threshold	$\beta = 4$ (≈ 6 dB)
CSA	Frame size	$N = 100$
	Repetition distribution	$L(x)$ = Soliton distributon $a = 0.02, k = 30$
Simulation	Number of simulations	100 or 1000
	Sample size of est. $\mathcal{C}_i$	1000000
Density Evolution	Maximum iterations	$I_{\max} = 100$

TABLE I: Reference parameters for evaluation

The Soliton distribution is that found in [15], parameterized by $a \in [0,1]$ and truncated to k terms: $L_2 = \frac{1}{L(1)}(\frac{1-a}{2})$ and for $3 \leq i \leq k$, $L_i = \frac{1}{L(1)}(\frac{1}{i(i-1)})$
For density evolution, $\rho(x)$ is deduced from $R(x)$, and $R(x)$ itself is a binomial distribution $B(N, \frac{r_{\text{avg}}}{N})$. $\frac{r_{\text{avg}}}{N}$ can be written as a function of the load g, our variable parameter in our evaluations, as $\frac{r_{\text{avg}}}{N} = g\frac{\ell_{\text{avg}}}{M}$. Hence the coefficients of $R(x)$:

$$R_j = \binom{N}{j}\left(g\frac{\ell_{\text{avg}}}{M}\right)^j\left(1-g\frac{\ell_{\text{avg}}}{M}\right)^{N-j}, 0 \leq j \leq j_{max}.$$

B. Impact of Wireless Propagation Parameters

We first analyze the impact of path loss on the performance of the system, which is the central topic of this article. The impact of the coefficient α is represented in Fig. 3, for two common values of the path loss exponent 3 and 4 and a high value of 5, and is compared to the situation without capture (nor SIR, e.g. $T_{\text{base}}(g)$ as found in [5]).

As expected, we can see that a higher path loss exponent, leads to higher throughput (due to interference having a more localized impact). The most dramatic observation is comparing the CSA with and without capture effect (e.g. T_{SIR} to T_{base}), where the throughput gain is around 2.5. This means that the capture effect must be taken into account.

Another observation is that the CSA with the Soliton distribution is rather close to the bound of Eq. (4): 78% to 81% of their bound, for the three values of α: this illustrates good performance. Indeed, under the conditions but without capture, the Soliton (in the same figure) reaches 69% of its bound $T_{\text{base}} = 1$, and we know that its asymptotic performance for the parameters that we selected $a = 0.02, k = 30$ would be $\frac{k}{k+1} - a \approx 95\%$ without capture (from [15]).

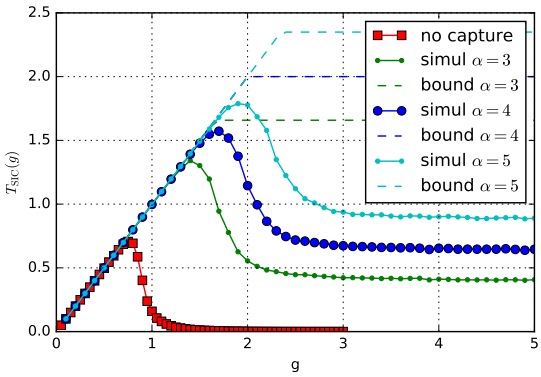

Fig. 3: Impact of path loss exponent α on throughput

Additionally, we observe that with capture the throughout converges towards some value > 0, unlike without capture where it converges towards 0. A known result for slotted ALOHA [18] that transposes to CSA (CSA operates at least as repetition coding slotted ALOHA even if no inter-slot SIC advances decoding; see also footnote 2).

Then we explore the impact of the capture threshold β on throughput, as shown in Fig. 4. As for α, β has a clear impact on performance, even more so for lower values of β ($\beta = 2$). Of course, β depends directly on the physical layer technology (not on the MAC protocol designer). Also, we note that for $\beta = 2$, the performance reached is even further from the bound Eq. (4). At this point, an open question is whether the protocol parameters (including the distribution and the frame size N) can be adjusted to reach (or get closer to) the upper bound.

C. Impact of CSA parameters

We investigate the impact of the frame size N, in our reference simulation. As we know from CSA literature, the results obtained by density evolution are asymptotic [5], [6],

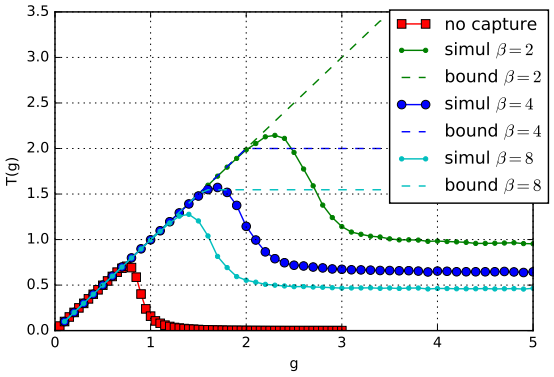

Fig. 4: Impact of capture threshold β on throughput

[16]. In order to find out how far is feasible to close the gap between the bound and the simulation, we propose to increase the frame size N. The results are shown in Fig. 5. As the frame size increases sixfold from $N = 100$ to $N = 600$, the performance goes from 79% of the bound to 93%. In other words, in this specific case, more than $2/3$ of the gap between the bound and the simulation can be accounted to the fact that we are in the non-asymptotic setting for the frame size.

In Fig. 6, we further increase the frame size N up to $N = 1600$ and plot the corresponding performance. We observe that we reach 96% of the lossless throughput bound. That indicates that in the non asymptotic regime with capture, we attain the same order of gain in throughput as in the asymptotic regime without capture (precisely 95% as previously evaluated).

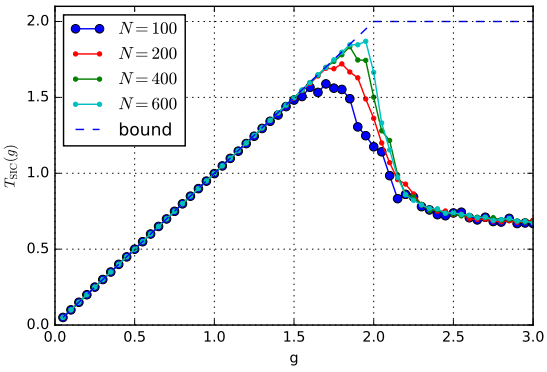

Fig. 5: Impact of the frame size N

It was found previously that the largest discrepancy between our simulations and upper bound was for a value of the capture threshold equal to $\beta = 2$ (and probably the gap would widen as β decreases). To see how close we could get in this case, simulations were performed and are represented in Fig. 7 (the bound in the figure is 3). We observe that the throughput increases from 72% for $N = 100$ to 83% for $N = 600$. From this, it is not possible to estimate how much CSA approaches the upper bound, but it seems that the limit would be lower.

In Fig. 8, we investigate the performance of different node distributions $L(x)$ defining the packets repetitions. "L3" stands for the distribution given in [5] as $L_3(x) = 0.5x^2 + 0.28x^3 + 0.22x^8$, with maximum throughput of 0.97 without capture. "d2", "d3" and "d4" are CRDSA [4] with 2, 3 and 4 repetitions and distributions x^2, x^3 and x^4 respectively. Finally "SA" denotes Slotted ALOHA and "LR2" is the second distribution given in [14] (obtained by numerical optimization with Rayleigh fading channel). The Soliton distribution and L_3 perform similarly, up to higher loads where the L_3 outperforms, in contrast to the CSA case without capture. Interestingly, the "LR2" distribution, optimized including the capture effect for a different system parameters(Rayleigh fading, target loss rate, etc.), dominates all other distributions with respect to throughput, including the Soliton. That indicates that under practical constraints the best distribution is yet to be found.

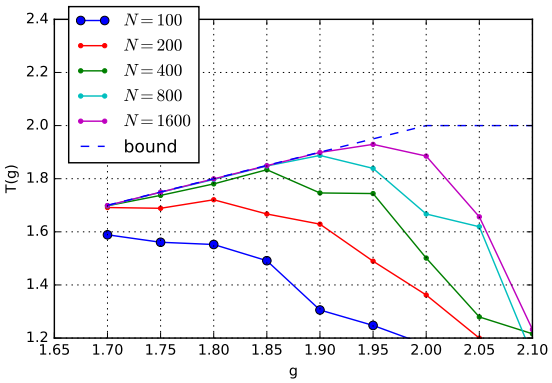

Fig. 6: Impact of the frame size N (zoom)

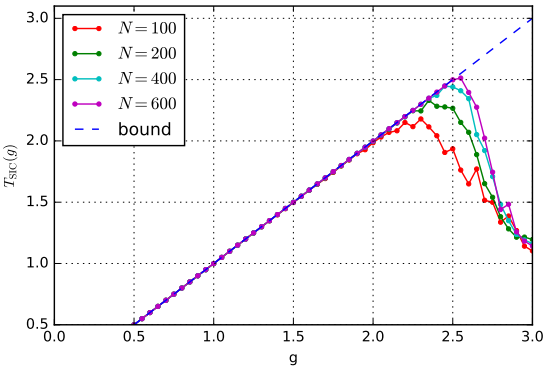

Fig. 7: Impact of the frame size N for $\beta = 2$

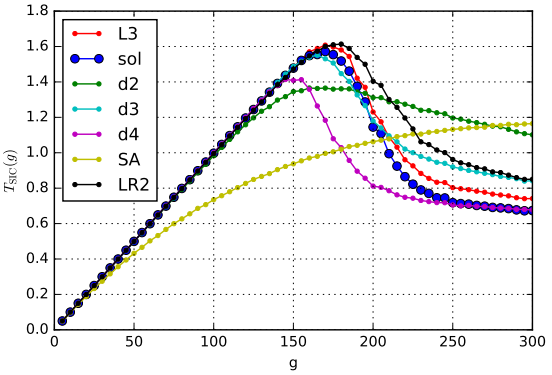

Fig. 8: Impact of the distribution of repetitions L

D. Density Evolution

Fig. 9 compares the result of the density evolution of Section III with simulations and the upper bound. We find that the DE models rather closely the simulation performance. Still, some discrepancies are found. Specifically at higher loads, the estimated throughput underperforms the simulation by about 33%; which is rather significant. In contrast, as shown in Fig. 5, the performance at high load varies very little depending on N, hence one should not expect such asymptotic behavior. Moreover, the maximum DE throughput is 1.84 (92% from the bound), which is below the maximum of 1.92 observed in Fig. 6 by 4%.

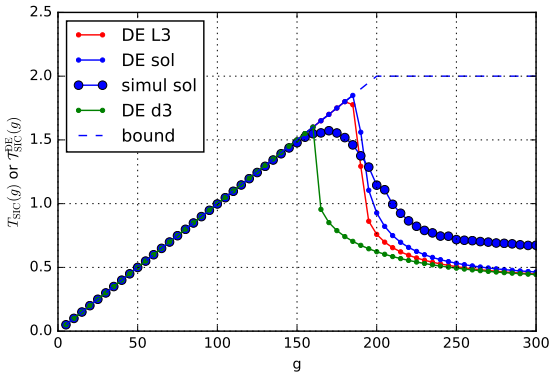

Fig. 9: Density Evolution vs simulations

While DE was considered as a reliable performance indicator without the capture , the latter effect causes inaccuracies to happen. That also may go beyond inaccuracies when comparing asymptotic versus non-asymptotic results. In line with our observations, it was highlighted in [13] that "The interdependencies among slots with respect to SIC are further amplified by the fact that in the assumed system model the received SNR of a particular user has the same value in all slots in which user transmitted". This claim holds for our scheme and indicates that the messages passed over the modeled graph are not independent, even asymptotically which further justifies our use of simulations as a primary tool for performance evaluation.

VI. Conclusion

In this paper, we presented an analysis, mostly empirical, of the Coded Slotted ALOHA protocol performance in wireless networks with path loss and capture effects. We also described evaluation methods (e.g. DE) and derived an analytical upper bound for lossless throughput.

The first result is the proof of gain by a factor of around 2.5 for CSA when capture is taken into account, with our default parameters. It is worth noting that this gain exceeds the gain of CSA over Slotted Aloha. We conclude that capture should be considered for an accurate analysis of CSA.

A second result, is the excellent behavior of the Soliton distribution; as it reaches 96% from the lossless throughput bound in Fig. 6, and conjointly demonstrates the excellent performance of CSA.Interestingly, the node distribution given in [14] was found to outperform the Soliton performance in the reference scenario, hence the best distributions under the practical constraints of the non asymptotic regime with capture is yet to be found.

Finally, we observe that the DE results are not perfectly accurate, making the refinement of DE methods with capture a topic to explore along with establishing more precise throughput bounds and the exploration of their achievability.

Acknowledgments

This work has been partially supported by the IFCPAR/CEFIPRA project "D2D Communications for LTE-Advanced Cellular Networks". The authors would like to thank Vinod Kumar, Chandra Murthy, Mohit Sharma, and other partners of the project, for discussions and insights on the topic. The authors would like to thank the anonymous reviewers for their constructive comments.

References

[1] Y. Polyanskiy, "A perspective on massive random-access," in *ISIT 2017*. IEEE, 2017.

[2] H. Nikopour and H. Baligh, "Sparse code multiple access," in *Personal Indoor and Mobile Radio Communications (PIMRC), 2013 IEEE 24th International Symposium on*. IEEE, 2013.

[3] C. Kahn and H. Viswanathan, "Connectionless access for mobile cellular networks," *IEEE Comm. Mag.*, vol. 53, no. 9, 2015.

[4] E. Casini, R. D. Gaudenzi, and O. D. R. Herrero, "Contention Resolution Diversity Slotted ALOHA (CRDSA): An Enhanced Random Access Schemefor Satellite Access Packet Networks," *IEEE Transactions on Wireless Communications*, vol. 6, no. 4, pp. 1408–1419, April 2007.

[5] G. Liva, "Graph-Based Analysis and Optimization of Contention Resolution Diversity Slotted ALOHA," *IEEE Transactions on Communications*, vol. 59, no. 2, pp. 477–487, February 2011.

[6] E. Paolini, G. Liva, and M. Chiani, "Coded Slotted ALOHA: A Graph-Based Method for Uncoordinated Multiple Access," *IEEE Transactions on Information Theory*, vol. 61, no. 12, pp. 6815–6832, Dec 2015.

[7] E. Paolini, C. Stefanovic, G. Liva, and P. Popovski, "Coded random access: applying codes on graphs to design random access protocols," *IEEE Communications Magazine*, vol. 53, no. 6, pp. 144–150, 2015.

[8] F. Baccelli and B. Blaszczyszyn, "Stochastic geometry and wireless networks: Volume i theory," *Foundations and Trends in Networking*, vol. 3, no. 34, pp. 249–449, 2010.

[9] S. Verdu, *Multiuser detection*. Cambridge university press, 1998.

[10] G. D. Nguyen, A. Ephremides, and J. E. Wieselthier, "On capture in random-access systems," in *Information Theory, 2006 IEEE International Symposium on*. IEEE, 2006, pp. 2072–2076.

[11] M. Zorzi and R. R. Rao, "Capture and retransmission control in mobile radio," *IEEE Journal on Selected Areas in Communications*, vol. 12, no. 8, pp. 1289–1298, 1994.

[12] X. Zhang and M. Haenggi, "The performance of successive interference cancellation in random wireless networks," *IEEE Transactions on Information Theory*, vol. 60, no. 10, 2014.

[13] Č. Stefanović, M. Momoda, and P. Popovski, "Exploiting capture effect in frameless aloha for massive wireless random access," in *Wireless Communications and Networking Conference*. IEEE, 2014, pp. 1762–1767.

[14] F. Clazzer, E. Paolini, I. Mambelli, and C. Stefanovic, "Irregular repetition slotted ALOHA over the Rayleigh block fading channel with capture," in *ICC*. IEEE, 2017.

[15] K. R. Narayanan and H. D. Pfister, "Iterative collision resolution for slotted aloha: An optimal uncoordinated transmission policy," in *Turbo Codes and Iterative Information Processing (ISTC), 2012 7th International Symposium on*. IEEE, 2012.

[16] G. Liva, "Graph-based analysis and optimization of contention resolution diversity slotted aloha," *IEEE Transactions on Communications*, vol. 59, no. 2, pp. 477–487, 2011.

[17] T. Richardson and R. Urbanke, *Modern coding theory*. Cambridge university press, 2008.

[18] C. Namislo, "Analysis of mobile radio slotted aloha networks," *IEEE Journal on Selected Areas in Communications*, vol. 2, no. 4, pp. 583–588, July 1984.